



The Society shall not be responsible for statements or opinions advanced in papers or in discussion at meetings of the Society or of its Divisions or Sections, or printed in its publications. Discussion is printed only if the paper is published in an ASME Journal. Papers are available from ASME for fifteen months after the meeting.

Printed in USA.

Copyright © 1989 by ASME

## Part-Circumference Casing Treatment and the Effect on Compressor Stall

N. A. CUMPSTY  
Whittle Laboratory  
University of Cambridge

### ABSTRACT

Results are presented and discussed from an axial compressor rotor operated with an axial skewed slot casing treatment over part of the circumference. The compressor was one for which stall was initiated in the tip region and for this type there is some potential for stall margin improvement with lower loss using this. The main significance of the experiments is, however, the possibility of looking at aspects of stall inception. Normally stall inception is a brief transient with an unknown start time and is difficult to study but with the partial casing treatment it was possible to make the untreated section operate continuously in such a way that it underwent the processes normally leading to stall. For a tip stalling rotor the experiments identify the annulus boundary layer as the crucial region of the flow and spillage of the tip-clearance flow forward of the blades as a process leading to the rapid build up of blockage prior to instability and stall.

### NOMENCLATURE

- $p_1, p_2$  static pressure on casing wall upstream and downstream of rotor
- $p_{01}$  stagnation pressure into rotor
- $U_m$  blade speed at mid span
- $v_x$  axial velocity
- $V_x$  axial velocity outside boundary layer
- $y$  distance in from casing wall
- $\delta^*$  displacement thickness based on axial velocity
- $\theta$  momentum thickness based on axial velocity
- $\rho$  density
- $\phi$  flow coefficient  $V_x/U_m$

$\phi_{\text{mean}}$  mean or average flow coefficient

$\psi_{\text{ss}}$  static pressure rise coefficient based on  $U_m$

### INTRODUCTION

The use of casing treatment over the tips of rotors has been shown to give considerable improvements in stall margin in many cases. Its use has been more restricted than this advantage might suggest because of the correlation between stall margin improvement and degradation in efficiency, see for example Fujita and Takata (1984). It was suggested that by using casing treatment over part of the annulus one might obtain worthwhile improvements in stall margin with acceptable (or at least smaller) losses in efficiency. The present tests set out to determine what changes in stall margin were possible with partial coverage of the annulus; no torque meter was fitted to the compressor and efficiency changes could not be determined.

The tests with partial treatment have a wider interest because of the ignorance surrounding both the way in which casing treatment achieves its effect and also the initiation and development of compressor stall. The casing treatment could be used to force the untreated part of the annulus to operate at a flow coefficient which would be low enough to stall it if there were no treatment. Steady observations could be made of processes which normally occur only as a transient. Earlier tests reported by Smith and Cumpsty (1984), using the same rig and the same type of casing treatment, axial skewed slots, had demonstrated that changes to the annulus boundary layer are crucial to the treatment effectiveness. The treatment produces a markedly smaller displacement thickness downstream of the rotor, with much reduced swirl. It seemed probable that something could be learnt of stall inception by examining the boundary layer development close to stall and how this changed in the circumferential direction.

Most of the present paper is concerned with measurement of the boundary layer when part of the circumference over the rotor tips was fitted with casing treatment. It is the outcome of student projects in 1981 and 1982 but because no satisfactory explanation could be found for the results they have not been reported until now. Recent observations of the transient behaviour leading to stall by McDougall(1988), which are also described by McDougall and Cumpsty(1989), give a reason now for presenting these measurements. Further the Navier-Stokes calculations carried out by McDougall give an explanation for one of the more puzzling of the observations.

### EQUIPMENT AND METHOD

All the tests were carried out using an isolated rotor 1.52 m (5 feet) in diameter running at 250 or 450 rev/min. The rotor had 22 blades of C4 section with 152 mm (6 inch) chord constant along the whole span and an aspect ratio of 3. At the tip the solidity was 0.7, camber 8°, stagger 60.7° and thickness-chord ratio 8%. The blading and the rig is described in more detail elsewhere, for example Hunter and Cumpsty(1982) or Smith and Cumpsty(1984). All the present tests were run with a tip clearance of about 2 mm.

The casing treatment was that used by Smith(1980), a skewed axial slot of a design given by Prince et al (1974). The slots formed rectangular cavities covering 73% of the blade axial chord, inclined at 60° to the radial direction, Figure 1. There were a total of 360 slots with a ratio of open area to total area ratio equal to 0.7.

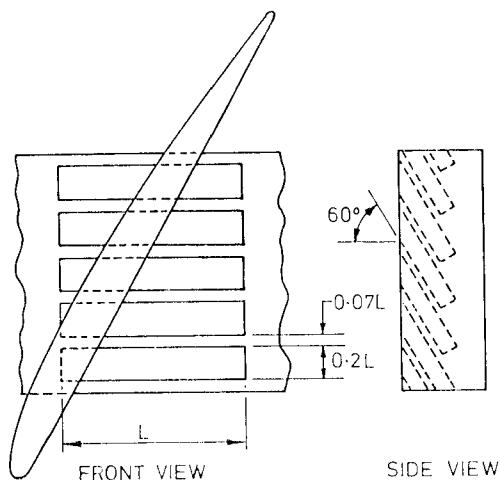


Figure 1. The axial skewed slot casing treatment

Measurements of total pressure and flow direction were made 11% of chord upstream and 24% of chord downstream of the rotor with a non-rotating three-hole cobra probe. This was used with the probe nulled to balance pressures in the outer holes. Although traverses were made right across the annulus, the majority of measurements were made in the boundary layer.

The present measurements were made with an artificially thickened inlet boundary (inlet displacement thickness,  $\delta_{in}^* = 11.7$  mm) whereas the Smith and Cumpsty (1984) measurements were made with the natural inlet boundary layer ( $\delta_{in}^* = 6$  mm). The thicker inlet boundary layer made the boundary layers easier to measure; it also made the static pressure rise across the rotor larger and gave a larger proportional reduction in  $V_x/U_m$  at stall when casing treatment was used.

Results are described using a flow coefficient  $\phi = V_x/U_m$  where  $V_x$  is the mean inlet axial velocity and  $U_m$  is the mean blade speed. (The rotor was designed a free vortex flow at  $\phi = 0.7$  and in an untreated build, that is with smooth casing walls, the rotor stalls at  $\phi \approx 0.40$ ). Static pressure rise across the rotor was determined from static tappings 0.93 chords upstream of the leading edge and 1.0 chord downstream of the trailing edge of the rotor. This positioning of the pressure tappings was a mistake because they were close enough to the rotor to be directly affected by it: the meridional streamline curvature across the rotor alters the wall static pressure and the blade-to-blade non-uniformity inevitably causes the mean static pressure to be recorded low. Pressure rises are expressed in terms of the static-to-static coefficient

$$\psi_{ss} = (p_2 - p_1) / (1/2 \rho U_m^2)$$

For all the tests described here the casing treatment was fitted and to achieve the effect of a smooth wall, self-adhesive tape was used to cover the slots. To carry out boundary layer traverses at a number of circumferential positions relative to region of the casing treatment it was only necessary to move the tape, keeping the traverse gear at the same circumferential position.

### OVERALL PERFORMANCE

Although most of the measurements were made at 450 rev/min, the overall pressure rise versus flow coefficient measurements were mainly made at 250 rev/min. This was because these tests involved repeated running into stall and with partial casing treatment this set up quite strong vibration which was felt to be damaging to the rig. The effect of the change in speed on flow coefficient at stall and on pressure rise was very small. For stall with full casing treatment :

$$450 \text{ rev/min} \quad \psi_{ss} = 0.86, \quad \phi = 0.33$$

$$250 \text{ rev/min} \quad \psi_{ss} = 0.843, \quad \phi = 0.34$$

(At 250 rev/min the Reynolds number based on the chord length and velocity at the tip was  $2.4 \cdot 10^5$ .)

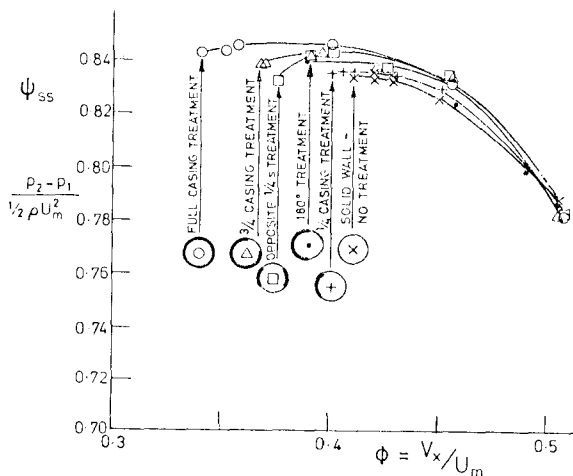


Figure 2. The static pressure rise coefficient at the casing wall versus flow for different partial casing treatment configurations. Inlet boundary layer displacement thickness 11.7 mm, 250 rev/min, Reynolds number  $2.4 \cdot 10^5$  based on tip chord,

Figure 2 shows the static-to-static pressure rise coefficient plotted against flow coefficient for the build with full casing treatment, and four intermediate cases with partial treatment. The left-most point for each curve is the nearest point to stall at which it was possible to run for a few minutes; the stall being stochastic it could occur at random and the smaller the flow coefficient the shorter the typical time for which unstalled operation would persist. In every build the casing treatment has reduced the flow coefficient at stall and raised the peak pressure rise. The results can best be understood by recognising that in a partial treatment configuration it is the extent of the untreated flow which determines stall. Thus the case when there was 270° of treatment (with 90° untreated) had almost the same stall point as the case with two opposite segments of treatment each of 90°.

The increase in static pressure rise does not in itself represent an improvement in efficiency and in this experiment without a torque-meter the efficiency could not be found. (It should be mentioned that when casing treatment is installed the rotor work cannot be calculated from the Euler work equation because of the torque reaction on the casing treatment itself.) One can expect nevertheless that the amount of efficiency penalty with casing treatment will depend largely on its circumferential extent of it and that with two sections of 90° there will be less additional loss than with full 360° treatment.

The configuration studied most had casing treatment covering a single arc of 180°. For this case the pressure rise versus flow rate is shown in Fig.3 together with the curves for no treatment and complete (i.e. 360°) treatment. This time the pressure rise shown is the difference between the downstream static pressure  $p_2$  and the inlet stagnation pressure  $p_{01}$ , the so-called total-to-static pressure rise. This pressure rise is of particular relevance because simple two-dimensional stability analyses predict that the flow becomes unstable when the gradient  $\partial(p_2 - p_{01})/\partial V_x$  is equal to zero. This is described by Stenning(1980) and in a

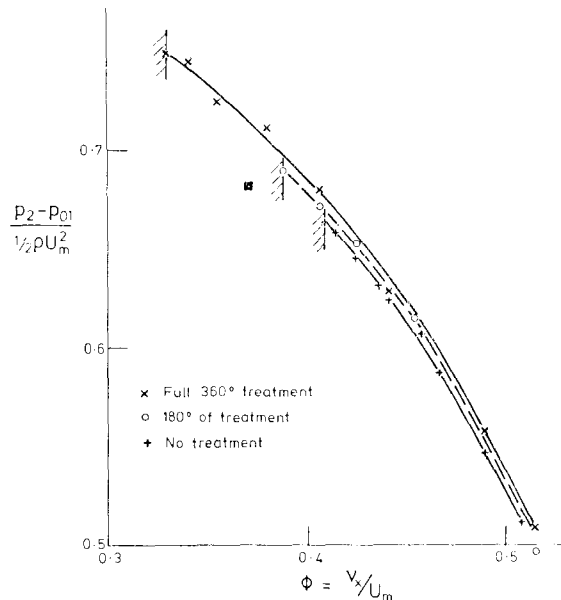


Figure 3. Coefficient of outlet casing static pressure minus inlet stagnation pressure versus flow for no casing treatment, 180° and 360° of treatment

wider context by Greitzer(1980). The present geometry is not well described as two-dimensional, having a hub-tip ratio of only 0.4, but qualitatively the idea is likely to be relevant. It is very apparent that the time mean curves shown do not approach the condition  $\partial(p_2 - p_{01})/\partial V_x = 0$  at the stall point and instability is not being initiated at the overall condition described by the simple theories.

Figure 4 shows the distribution of non-uniform static pressures measured around the casing wall for the build with 180° of treatment at a mean flow coefficient very close to stall,  $\phi_{mean} = 0.39$ . There is a very pronounced circumferential pattern both upstream and downstream, but it must be noted that there is a large mean difference separating the positive pressure downstream from the negative pressure upstream. (The absolute mean level on the upstream side has been adjusted to be compatible with the known flow rate; the circumferential variation has not, however, been altered and is believed to be correct.) Although not shown the amplitude of the pressure variation decreased very rapidly as the mean flow rate was increased from the value for stall. It can also be seen that the pressure variation decreases in amplitude as one moves upstream with the higher spatial frequencies decaying more rapidly. The upstream static pressure on the casing (and similarly the local axial velocity) and the downstream static pressure are functions not only of the mean flow coefficient  $\phi_{mean}$  but also of the circumferential position and the axial distance from the blade.

In the upstream region the flow is essentially a steady potential flow which is non-uniform because of the different rotor performance produced with and without casing treatment. By standard techniques for a two-dimensional flow the amplitude of pressure variation can be used to calculate the variation in flow direction compatible with it, see for example Katz(1958). The

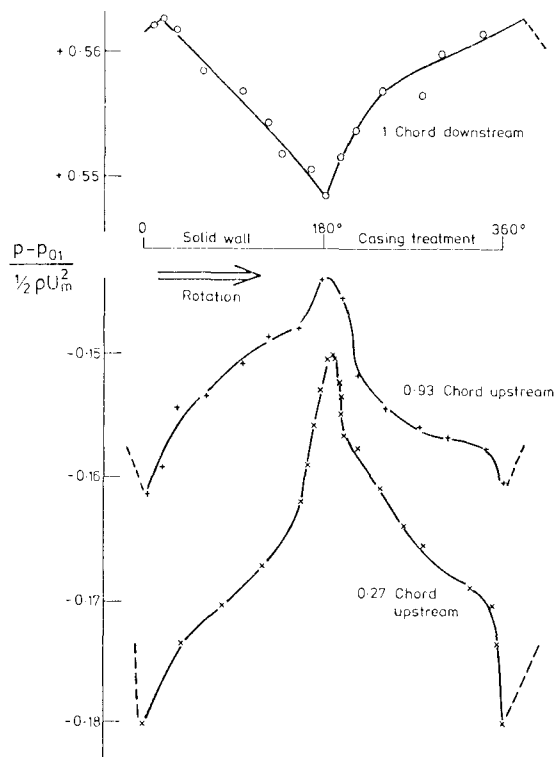


Figure 4. The static pressure variation around the circumference with 180° of casing treatment at  $\phi_{mean}=0.39$  (very close to stall). Note very large difference between upstream and downstream magnitudes (absolute values of upstream pressure unreliable).

was a result of the boundary layer variation, discussed below, rather than the cause.

The boundary layer measurements described below point to the region near the end of the untreated section as initiating stall and from Fig. 4 it is possible to arrive at the local conditions very close to stall. Because the section with casing treatment inhibits the stall the flow in the untreated section is held in a condition which would normally lead to the rapid transient which is the breakdown into stall. With uniform inlet stagnation pressure the variation in upstream static pressure distribution can be translated into the variation in local axial velocity. It is easy to show that the perturbation in axial velocity is given by

$$\delta V_x / U_m = \delta p_1 / (\rho U_m^2) (1 / \phi_{mean})$$

and since  $\phi_{mean} \approx 0.4$  it follows that

$$\delta V_x / U_m \approx 1.2 \delta p_1 / (1/2 \rho U_m^2)$$

Where the inlet static pressure is highest, at the end of the untreated section, the axial velocity will be lowest. At the end of the untreated region the local axial velocity is lower than the mean by about 5%, in other words locally  $V_x / U_m = 0.37$ .

On the downstream side the lowest static pressure occurs at the end of the untreated region in Fig.4 and is approximately  $0.007(1/2\rho U_m^2)$  below the mean. As noted above it is the difference  $p_2 - p_{01}$  which is relevant to the consideration of stability and in the present work the inlet stagnation pressure may be taken to be constant.

Figure 3 shows the mean pressure rise  $p_2 - p_{01}$  versus the annulus average  $V_x / U_m$ . To arrive at the local conditions at the end of the untreated region very close to the stall point the perturbations found in the above paragraphs should be subtracted from the mean. If the value  $0.007(1/2\rho U_m^2)$  is subtracted from the average pressure rise for the point nearest to stall in Fig.3 and the flow rate is reduced by 5% below the average value the point representing local conditions very close to stall at the end of the untreated region is obtained. This is shown in Fig.3 by a solid square point. The amplitude of the non-uniformity decreases very rapidly as the mean flow rate is increased and deviation of the local performance from the curve for the mean would rapidly disappear. The shape of curve for the performance near the end of the untreated region is therefore altered significantly only in the region near to stall. Without too much difficulty the analytic condition for instability,

$$\partial(p_2 - p_{01}) / \partial V_x = 0,$$

could be imagined to be locally fulfilled by considering the curve through the solid point merging in with the undisturbed curve at higher flow rates.

#### BOUNDARY LAYER MEASUREMENTS

Before presenting and discussing individual boundary layer profiles, it is appropriate to present the overall results in terms of integral thickness. Only those relating to the axial profile are considered here. These are the displacement thickness :

$$\delta^* = \int_0^\delta \left\{ 1 - \frac{v_x}{V_x} \right\} dy$$

and the momentum thickness :

$$\theta = \int_0^\delta \left\{ 1 - \frac{v_x}{V_x} \right\} \frac{v_x}{V_x} dy$$

obtained by integrating to the boundary layer edge. The determination of the overall thickness,  $\delta$ , and the "free-stream" velocity  $V_x$  is inherently somewhat arbitrary for a flow as complicated as the annulus wall boundary downstream of the rotor. The approach adopted here is to take  $\delta$  to be where the axial velocity reaches its maximum value. Upstream of the rotor the same difficulty did not arise as the maximum velocity also corresponded to the total pressure becoming uniform (as in conventional boundary layer theory). The upstream boundary layer about one chord upstream of the rotor was sensibly constant for all the tests and is characterised by  $\delta^* = 11.7$  mm,  $\theta = 9.2$  mm.

For the solid wall and for the full casing treatment build the flow is nominally axisymmetric. For these builds the following integrals were measured

Downstream boundary layer thicknesses, mm

	$\phi$	$\delta^*$	$\theta$	
Solid wall	.415	10.9	7.7	stall point
Full treatment	.415	5.0	3.9	
" "	.391	6.4	4.8	
" "	.377	7.7	5.6	
" "	.34	11.3	7.1	stall point

It is notable that the overall integral thicknesses were very similar at the stall point in these two uniform cases. It points to the annulus boundary layer as being a limiting quantity in both cases.

Displacement thicknesses measured at different circumferential positions with 180° of treatment are shown in Figure 5 at two flow coefficients, one very close to stall, the other not far away. The larger flow,  $\phi = .41$ , corresponds to very close to the stall point of the solid wall build, whereas  $\phi = 0.39$  corresponds to close to stall of the 180° build for which the measurements apply. The solid wall section covers from 0 - 180° and over this range the boundary layer thickness increased after an initial dip. The rate of increase was very much more rapid close to the stall point of the build. Over the casing treatment the thickness decreased and rapidly settled down to values almost equal to those for full treatment at the same flow coefficient.

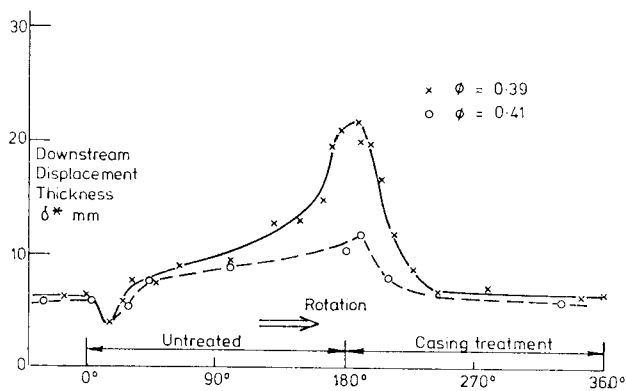


Figure 5. Displacement thickness downstream of rotor measured around the circumference with 180° of casing treatment for  $\phi_{\text{mean}}=0.39$  (very close to stall) and  $\phi_{\text{mean}}=0.41$

Closer inspection of Fig. 5 shows that the minimum thickness occurred over the solid wall (at about 16°) and the maximum thickness occurs over the casing treatment at between 180° and 190°. Part of the explanation for this is that the swirl from the rotor carried the effects tangentially around from the edge of the casing when moving the axial distance between rotor trailing edge and cobra probe.

Figure 6 shows the variation in downstream displacement thickness for treatment comprising two sections of 90° at the flow coefficient close to stall for this build,  $\phi = 0.377$ . Superimposed are some results taken with 270° of treatment, also at  $\phi = 0.377$ , the untreated 90° overlapping the previously mentioned results. Just as for the 180° of treatment shown in Fig.5, the maximum and minimum thickness with 90° treatment occurred after the end of the untreated and treated walls respectively. The results for 90° of treatment, unlike those with the 180° treatment, show the flow in the treated section no longer returning to a steady value and in this case the flow over the treatment still appeared to be in the process of recovering when it reached the end of the treatment. It is not just that the extent of the casing treatment was less, but the flow recovered more slowly, over about 90° instead of about 50°, presumably because being closer to the stall point of the compressor with full casing treatment there was less performance margin to correct the increased thickness.

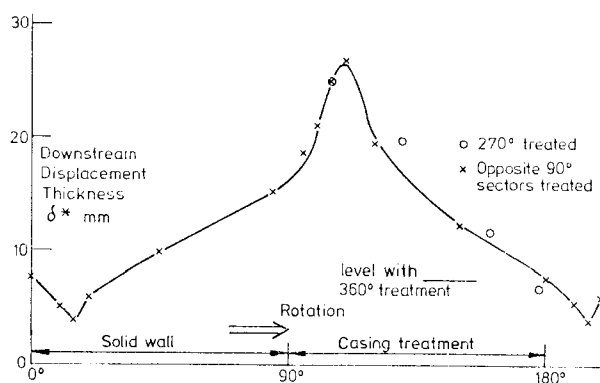


Figure 6. Displacement thickness downstream of rotor measured around the circumference with 270° of treatment and with two sections of 90°,  $\phi_{\text{mean}}=0.373$  (very close to stall)

Superimposed on the results with two 90° sections of treatment in Fig.6 are measurements of the downstream displacement thickness with 270° of treatment, the untreated section being overlaid in the figure. The boundary layer variation was similar in both cases.

The circumferential variation in thickness presents a problem of interpretation. It is convenient to talk of the boundary layer growing around the circumference or the flow recovering around the annulus, and this has been done above, but it is not clear in what way this takes place. Early attempts to explain this focused on the pressure variation creating the boundary layer variation and this led to the upstream boundary layer being measured. Figure 7 shows the displacement and momentum thicknesses upstream and downstream of the rotor with 180° of treatment at a flow rate very close to stall. This shows the remarkable feature that the very high local levels of thickness near the end of the solid region were present

upstream of the rotor. Also the axial momentum thicknesses were generally lower downstream than upstream, implying that the axial blade force was actually higher in the boundary layer than in the free-stream; only where the boundary layer thickness is a peak was this no longer true.

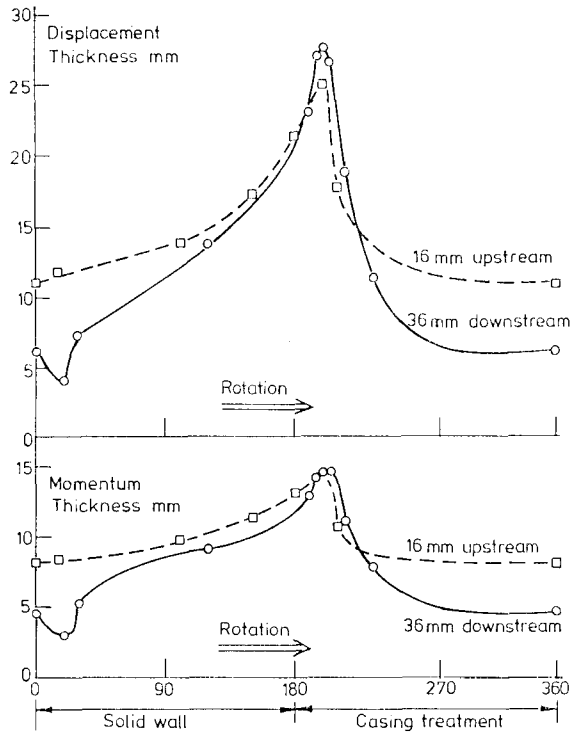


Figure 7 Displacement and momentum thickness upstream and downstream of rotor measured around circumference with 180° of treatment,  $\phi_{mean}=0.39$  (very close to stall)

The exceptionally high values of boundary layer thickness which occurred upstream of the rotor towards the 180° position require explanation. Initially it was thought that it might be caused by the non-axisymmetric pressure field but calculations showed that the pressure field was orders of magnitude too small to have this effect. It was concluded that only by having flow spill forward from the blades close to the casing could this occur but in 1982 this was no more than unsupported conjecture. Recently McDougall(1988) has used a Navier-Stokes calculation method developed by Dawes(1987) to examine the flow around highly staggered rotor tips at flow rates below those for design. An important feature is the flow out of the tip clearance. At flow coefficients not far from the design value the clearance jet is predicted to move out roughly normal to the blade chord before being turned and rolled over to pass down the blade passage. Measurements of the flow leaving the blade passage have confirmed this pattern. At lower flow coefficients the calculation showed the clearance jet to be stronger and to progress further upstream so that when it is rolled over it passes ahead of the next blade and spills into the next passage further along. It is believed that this is what was occurring with the flow leading to Fig.7: where there was no casing treatment

the tip-clearance flow from one passage spilled to the next. The spilled flow exacerbated conditions in the next passage so more flow could spill to the next and so on. It also seems very probable that large tip-clearance flows could cause the spilled flow from an earlier passage to be inhibited from entering causing cumulatively greater amounts of spilled flow to move circumferentially ahead of the rotor. Relative to the rotor the clearance flow moves backwards but in the absolute frame of reference it moves in the same sense as the rotor.

In a conventional axisymmetric geometry there would be no way in which this process could be viewed as a steady process. McDougall(1988) did see evidence with hot wires just upstream of the rotor for the spilled flow as stall was initiated, but it was a brief transient. The partial casing treatment has captured the process as a steady one.

**THE MECHANISM OF STALL**

This section contains ideas which are conjecture on the evidence presented in this paper, but taken with the work of McDougall(1988) it may be given some weight. The compressor on which these ideas are based was known to have stall initiated in the tip region, and only for such machines are these ideas of any validity. It may also have some application to unshrouded centrifugal compressors, particularly to those with axial inducers, although work by Fink(1988) shows that many such compressors have strong circumferential variations resulting from the tongue of the scroll.

It seems clear that with treatment around part of the circumference the spillage of clearance flow in the untreated section led to a build up of blockage on the upstream side of the rotor. The blockage led to a reduction in the static pressure rise in the blade passages affected, so that towards the end of the untreated region the outlet static pressure was measurably lower. The lower static pressure at outlet was sufficient to allow the flow to be locally unstable by the criterion  $\partial(p_2-p_{01})/\partial V_x=0$ . In the absence of a region of casing treatment the unstable flow would rapidly change into a stalled flow but the sector of casing treatment prevented this in two ways. First the flow was stable in the treated region so that the waves travelling out from the unstable region became attenuated. Second it put a stop on the growth of the inlet blockage being caused by the spillage. It is believed that an important part of the operation of casing treatment is the inhibition or elimination of the spillage of clearance flow ahead of the blades.

In a normal axisymmetric configuration, with or without casing treatment, it seems probable that as stall is approached spillage leads to a serious build up of blockage ahead of the blades and thus to a local reduction in the pressure rise. It seems likely that in this case too the flow will become unstable where the downstream static pressure is low only over a small fraction of the annulus. Stall will be initiated there, as in the partial casing treatment case, when the remainder of the annulus is no longer able to bring the attenuation of the disturbances resulting from the unstable region. This is a rapid transient process in an axisymmetric configuration.

Downloaded from http://asmedigitalcollection.asme.org/GT/1989/79139V001T01A1102398625V001101A110-89-gf-312.pdf by guest on 20 August 2022

## CONCLUSIONS

There seems to be some benefit in having small segments with casing treatment and some without as a way of reducing the drop in efficiency but gaining most of the stall margin improvement.

The use of a deliberately non-axisymmetric configuration leads to a useful vehicle for studying stall and testing ideas; partial casing treatment is a good way of achieving this. It seems very likely that with the progress in understanding of stall initiation that has occurred in the last 8 years a very useful experimental program could be undertaken.

An important process that takes place in axial compressors at flows below design is the spillage of the tip-clearance flow. The evidence obtained from this work is that the spilled flow can build up circumferentially to give locally very high inlet blockage on the annulus wall. This was observed in a steady manner using partial casing treatment but it also seems to be a mechanism of flow breakdown in other compressors which stall at the tip. Where this occurs it is possible for the outlet static pressure to be locally reduced enough for instability to occur. If this is true it explains the common observation that the stall point often occurs when the average, time-mean value of  $\partial(p_2-p_{01})/\partial V_x$  is well away from zero, the value believed necessary for the flow to be unstable. It is not necessary for flow to satisfy this criterion either in the time-mean or area-mean sense, but only locally as a transient.

## ACKNOWLEDGEMENTS

This paper is based on experimental work carried out as final year undergraduate projects in the Whittle Laboratory in 1981 and 1982. Thanks are therefore expressed to Messrs. S.Z.Anwar, D.M. Apthorp, J.M.Copley and P Hemsley. In the preparation of the paper the assistance of discussion with Professor E.M. Greitzer is appreciated: this was made possible by a NATO travel grant.

## REFERENCES

- Dawes, W. N., 1987 "A numerical analysis of the three-dimensional viscous flow in a transonic compressor rotor and comparison with experiment." *ASME Journal of Turbomachinery* Vol. 109, pp. 83-90
- Fink, D.A., "Surge dynamics and unsteady flow phenomena in centrifugal compressors." Ph.D. Thesis, Massachusetts Institute of Technology
- Fujita, H. and Takata, H. 1984 "A study of configurations of casing treatments for axial flow compressors." *Bulletin of Japan Society of Mechanical Engineers*, Vol.27, pp1675-1681.
- Greitzer, E.M., 1980 "Review - Axial compressor stall phenomenon." *ASME Journal of Fluids Engineering* Vol. 102, pp.134-151
- Hunter, I.H. and Cumpsty, N. A., 1982 "Casing wall boundary layer development through an isolated rotor." *ASME Journal of Engineering for Power* Vol. 104, pp. 805-817
- Katz, R., 1958 "Performance of axial compressors with asymmetric inlet flows." *Report, Daniel and Florence Guggenheim Jet Propulsion Center, California Institute of Technology.*
- McDougall, N. M., 1988 "Stall Inception in Axial Compressors." Ph.D. Dissertation, University of Cambridge.
- McDougall, N. M. and Cumpsty, N. A., 1989 "Stall inception in axial compressors". *A paper submitted to the 34th ASME Gas Turbine and Aeroengine Congress and Exposition*
- Prince, D. C., Wisler, D. C. and Hilvers, D. E., 1974 "Study of casing treatment stall margin improvement phenomenon." NASA CR 134552
- Smith, G. D. J., 1980 "Casing Treatment in Axial Compressors." Ph.D. Dissertation, University of Cambridge
- Smith, G. D. J. and Cumpsty, N. A., 1984 "Flow phenomena in compressor casing treatment." *ASME Journal of Engineering for Gas Turbines and Power* Vol. 106, pp.532-541
- Stenning, A. H., 1980 "Rotating stall and Surge." *ASME Journal of Fluids Engineering* Vol. 102, pp.14-20